Original Article
Inhibiting the mobilization of Ly6C^{high} monocytes after acute myocardial infarction enhances the efficiency of mesenchymal stromal cell transplantation and curbs myocardial remodeling

Wenbin Lu[1,2*], Yong Tang[1,2*], Ziwei Zhang[1], Xiaofeng Zhang[1,2], Yuyu Yao[1], Cong Fu[1], Xin Wang[1], Genshan Ma[1*]

[1]Department of Cardiology, Zhongda Hospital Affiliated with Southeast University, China; [2]Department of Cardiology, The Second Hospital Affiliated with Southeast University, China. *Equal contributors.

Abstract: Background: Ischemia related inflammation is the most critical factor for the survival of transplanted mesenchymal stem cells (MSCs), and strategies for controlling excessive inflammation after acute myocardial infarction (AMI) are essential and necessary for cell transplantation therapy. Our present study tested the effect of decreased Ly6C^{high} monocytes on mouse MSCs transplantation after AMI. Methods: BALB/c AMI mice were treated systemically with a CCR2 antagonist (RS 504393, 2 mg/kg, subcutaneously) or normal saline (control group). Next, 10^5 EdU-labeled MSCs were administered by intramyocardial injection to the mice in each group. TUNEL kits were used to identify the apoptotic cardiomyocytes in the infarct. The slides of the infarct border zone were stained with wheat germ agglutinin to measure the vessel density, and anti-myosin heavy chain eFluor 660 was used to measure the cardiac myosin-positive area. A transwell chamber was used to examine the interactions between Ly6C^{high} monocytes and MSCs. The inflammatory cytokines expressed by Ly6C^{high} monocytes and the SDF-1 expressed by MSCs were detected using ELISA kits. MSC viability was further examined by MTT and mitochondrial membrane potential assays by flow cytometry using JC-1 kits. Results: We first observed the increased survival of transplanted MSCs (11.2 ± 3.4/mm^2 vs. 3.5 ± 1.6/mm^2, p < 0.001), and the decreased apoptosis of cardiomyocytes ($11.20\% \pm 3.55\%$ vs. $20.51\% \pm 8.17\%$, p < 0.001) in the infarcts at 3 days in the CCR2 antagonist group. An increased number of capillaries and small arterioles (139.6 ± 21.7/mm^2 vs. 95.4 ± 17.6/mm^2, p < 0.001) and an increased cardiac myosin-positive area ($17.9\% \pm 6.6\%$ vs. $11.8\% \pm 3.5\%$, p < 0.001) were also observed in the infarct zone at 21 days post MSC infusion in the CCR2 antagonist group. In addition, a significantly increased LvEF% (50.17 ± 10.06 vs. 45.44 ± 9.45, p < 0.001) was detected at the same time compared to the control mice. We further demonstrated that both the mitochondrial membrane potential of the MSCs (0.45 ± 0.11 vs. 3.4 ± 0.3, p < 0.001) and stromal cell-derived factor-1 (SDF-1) secreted by the MSCs significantly decreased (80.77 ± 39.02 pg/ml vs. 435.5 ± 77.41 pg/ml, p < 0.001) when co-cultured with Ly6C^{high} monocytes. This is possibly mediated by the over-expressed cytokines secreted by the Ly6C^{high} monocytes compared to the Ly6C^{low} monocytes, including IL-1 (139.45 ± 30.44 vs. 80.05 ± 19.33, p < 0.001), IL-6 (187.82 ± 40.43 vs. 135.5 ± 22.09, p < 0.001), TNF-α (121.77 ± 31.65 vs. 75.3 ± 22.14, p < 0.001) and IFN-γ (142.46 ± 27.55 vs. 88.25 ± 19.91, p < 0.001).

Keywords: Ly6C^{high} monocytes, MSCs, AMI, CCR2

Introduction

Coronary artery disease (CAD) is likely the major cause of heart failure in both developed and developing countries [1]. Stem cells, such as bone marrow derived mesenchymal stem cells (MSCs), have been used to treat atherosclerotic heart disease and other diseases that involve acute injury of myocardium [2-4]. An attractive feature of MSCs is the lack of major histocompatibility complex (MHC) class II, rendering these cells relatively tolerant of immunological reactions. The paracrine effects of transplanted MSCs, including the secretion of a broad range of bioactive molecules, such as SDF-1, are now hypothesized to be the primary mechanisms by which MSCs achieve their therapeutic effect. However, previous

attempts to use these cells have not been particularly successful [5]. Despite the advantages of MSC transplantation for heart disease, detailed in vivo observations have shown that the MSC survival time was short post-MSC transplantation due to harsh microenvironments that include ischemia, inflammation and anoikis in the infarcted myocardium. Strategies to improve the cell viability of transplanted MSCs are necessary to improve cardiac function after cell transplantation therapy. Spleen derived monocytes, particularly Ly6C^high subsets are primarily involved in counteracting wound healing and contribute to left ventricular dilatation in acute myocardial infarction (AMI) [6, 7]. Our present study tested the hypothesis that the inhibition of the mobilization of Ly6C^high monocytes decreases the accumulation of cells in the infarcts, improves the efficacy of MSC transplantation and attenuates myocardial remodeling.

Materials and methods

AMI mice models and inhibition of CCR2

An anterior wall MI was induced by direct ligation of the left anterior descending (LAD) artery as previously described [8]. After anesthetization with pentobarbital sodium (50 mg/kg), the mice were endotracheally intubated and ventilated with room air at 110 breaths per minute using a rodent ventilator (Harvard Apparatus). A left thoracotomy was performed to expose the LV of the heart. The LAD coronary artery was visualized and ligated just below the left auricular level with an 8-0 nylon suture. Blanching and dysfunction of the anterior wall verified LAD ligation. The animal procedures were performed according to a protocol approved by the Institutional Animal Care and Use Committee (IACUC) at Southeast University.

For the pharmacological inhibition of CCR2 after AMI, the specific CCR2 antagonist, RS 504393, (Tocris, Bristol UK) was used (2 mg/kg, subcutaneous). The IC50 for CCR2 is 110 nmol/L. RS 504393 inhibits CCL2-induced chemotaxis with an IC50 of 360 nmol/L.

MSCs preparation, labeling and delivery

MSCs were isolated and cultured using standard protocols [9]. Femurs and tibias of 7- to 10-week-old mice were flushed using standard PBS (HyClone) to collect the bone marrow cells. FACS™-Lysing solution (BD Biosciences) was used to deplete the erythrocytes. After centrifugation at 1000 rpm/min for 5 min, the cells were washed 3 times and then resuspended in minimal essential medium supplemented with 10% FBS (DMEM, Gibco) at a density of 5×10^6 cells/cm^2. Non-adherent cells were removed at day 3, and the cells reached confluence after 2 weeks. Trypsin (0.25%) containing EDTA (HyClone) was used for the subsequent passaging. The monoclonal antibodies for Sca-1, CD105, CD90, CD31, CD34, and CD45 conjugated to FITC were used to identify the cells by flow cytometry (Becton Dickinson Inc. USA). The MSCs used for the experiments were from passages 5 to 6. Two days before infusion, the cells were freshly plated at a 1/3 ratio and incubated in complete medium with 10 μm/L [10, 11] EdU (5-ethynyl-2-deoxyuridine, Invitrogen) for 48 hours to label the cells. Incorporation of EdU was detected by reaction with azide-conjugated Alexa Fluor 488. The AMI mice described above received 10^5 MSCs resuspended in 100 μl of PBS via intramyocardial injection.

Isolation of monocytes and co-culture

The monocytes were obtained as follows: First, 6-8-week-old BALB/c mice were sacrificed. The belly skin was then opened by pulling the skin apart on the left side of the abdomen, and the abdominal membrane was not broken until the spleen was excised. After organ harvest, single cell suspensions were obtained from the spleen by digestion with a cocktail of 450 U/ml collagenase II, 125 U/ml collagenase IV and 60 U/ml hyaluronidase (Sigma-Aldrich) for 30 min at 37°C with shaking. After filtration through a 200-mesh screen and centrifugation at 400 × g, the cells were positively selected using CD11b MACS beads (Miltenyi Biotec) and then stained with anti-Ly-6C Abs. The purified cells were cultured in RPMI medium 1640 supplemented with 10% FCS in 6-well plates. The monocytes used for the experiments were from passages 3 to 6. Transwell chambers (Corning) were used to examine the interactions between the monocytes and MSCs (co-culture for 24 h). Inflammatory cytokines, including IL1/6, TNF-α and IFN-γ, in the supernatant of the Ly6C^high/low monocytes were further detected using ELISA kits (R&D).
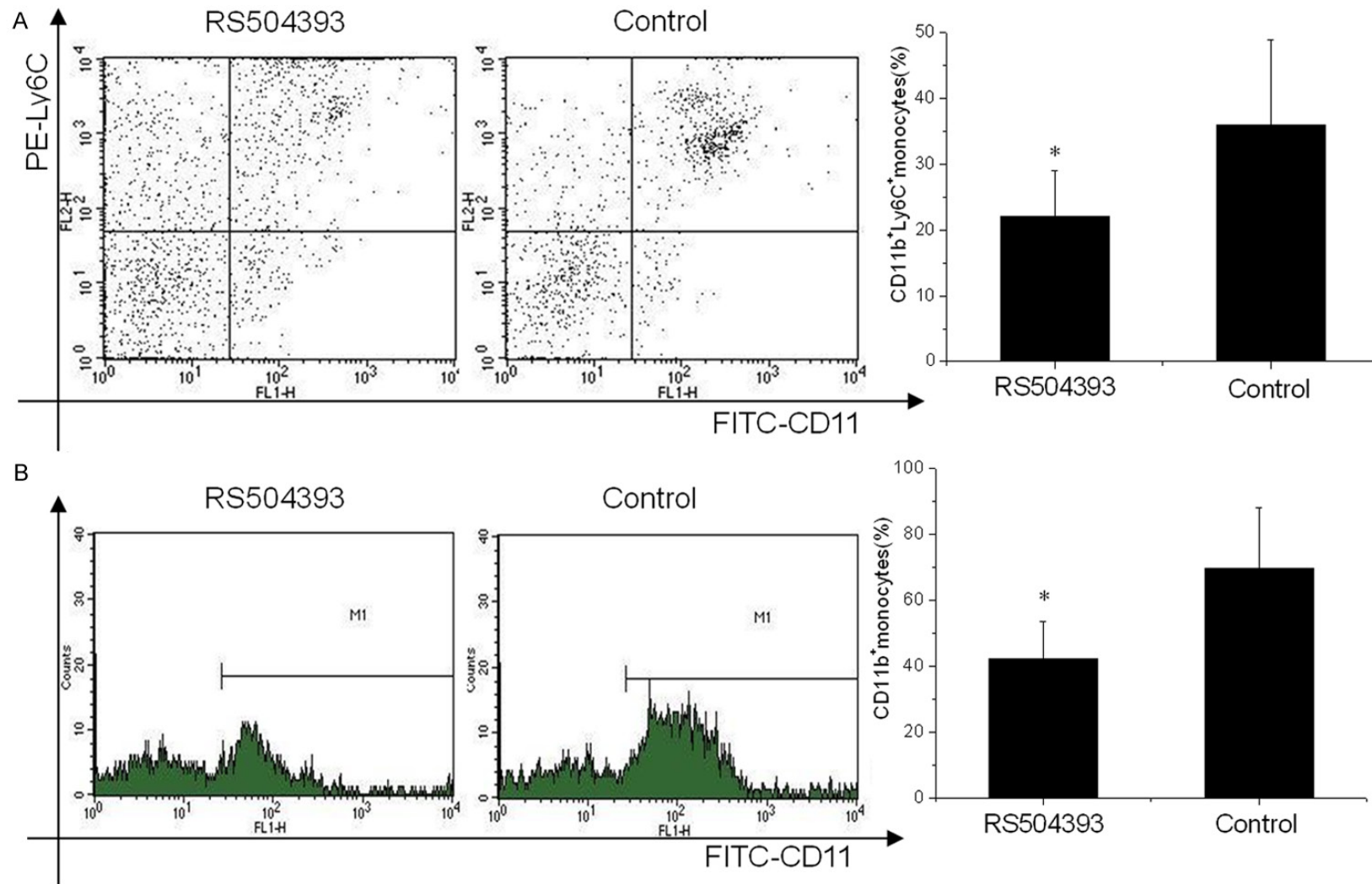
Figure 1. The effect of CCR2 inhibition on inflammatory infiltration post AMI (n = 20). A. Flow cytometry revealed different patterns of CD11b^{+}Ly6C^{high} cells in the circulation of AMI mice one day after treatment with RS504393. Significantly reduced cells counts were observed in the RS504393 group. B. Flow cytometry revealed reduced CD11b positive cells (monocytes and monocytes derived macrophages) in the infarct zone of AMI mice one day after treatment with RS504393. *p < 0.05 vs. the corresponding control group.

Real-time PCR

Three days after AMI, the hearts were perfused with saline, and the infarcted left ventricles were removed below the ligation. The total RNA was extracted from the infarct with Trizol reagent according to the manufacturer's instructions (Invitrogen). A QuantiTect Reverse Transcription Kit (Fermentas) was used for reverse transcription. Polymerase chain reaction was performed using Platinum SYBR Green qPCR SuperMix UDG (Applied Invitrogen) in a BIO-RAD MJ Mini Opticon Real-Time PCR System. The primer sequences were as follows: SDF-1 (NM_021704) 5'tgcccttcagattgttgcac3' and 5'ccacggatgtcagccttcc3'; and angiopoietin-1 (NM_001286062.1) 5'cattcttcgctgccattctg3' and 5'gcacattgcccatgttgaatc3'.

Immunostaining

The animals were sacrificed 3 days or 3 weeks after AMI. The tissues were fixed in formalin and embedded in paraffin blocks according to established protocols. The fixed hearts were serially cut 8 μm from the apex to below the coronary artery ligation site. After antigen retrieval, the specimens were incubated with 1% normal blocking serum in PBS for 60 min to suppress the nonspecific binding of IgGs. The slides were then incubated for 30-60 min with each mouse antibody or fluorescent reagents.

Three days after AMI, the infarction tissue was stained for EdU (Invitrogen) to calculate the live MSCs, and TUNEL kits (R&D Systems) were used to identify the nuclei of the apoptotic cardiac myocytes in the infarct border zone. Three weeks after AMI, the infarct border zone was stained with Texas Red-X conjugated wheat germ agglutinin (WGA, Invitrogen) to measure the vessel density. The tissue was further stained with anti-myosin heavy chain eFluor 660 (eBioscience) and 4,6-diamidino-2-phenylindole (DAPI, Roche) to measure the percent cardiac myosin-positive area in the infarct zone using Image Pro Plus software. Fluorescence microscopy (Olympus BX61) or a confocal laser scanning (CLS) microscopy system (Thorlabs, Inc.) was used as necessary for image acquisition of the immunostaining.

Flow cytometric analysis

One day after AMI, mouse blood was obtained and the monocytes were isolated through gradient density centrifugation following erythrocyte lysing. After two washes with cold PBS, the cells were resuspended at a concentration of 10^6 cells/ml. Single-cell suspensions were then incubated with FITC-rat anti-mouse CD11b and PE-rat anti-mouse Ly-6C (BD Biosciences). The CD11b$^+$Ly6C^{high} circulating monocytes and the CD11b$^+$ monocytes in the infarcts were further identified using a FACS Calibur cytometer (Becton Dickinson). The mitochondrial membrane potential of the co-cultured MSCs was also determined using the FACSCalibur cytometer with JC-1 mitochondrial membrane potential assay kits (Abnova).

Echocardiography

At one and twenty-one days after AMI, 2-dimensional echocardiography was performed on the mice using a Vevo 770^{R}high-resolution Imaging System (Visual Sonic, Canada) and Vevo analysis software (Vevo 2.2.3) as previously described [12, 13]. The LV dimensions and LV posterior wall thickness were quantified via digitally recorded 2-dimensional clips and Mmode images in a short axis view from the mid-LV just below the papillary muscles to allow for consistent measurements from the same anatomical location in each mouse. Each measurement in each mouse was repeated five to six times and performed using 3 randomly chosen m-Mode clips of the 5 recorded by the observer, who was blinded to the experiment group. The shortening fraction (FS) was calculated as (LvEDD-LvESD)/LvEDD × 100%.

Statistical analysis

Data management and statistical analysis were performed with Statistical Package for Social Sciences software (SPSS 18.0 for Windows, SPSS Inc.). Data are expressed as mean ± standard deviation. Categorical variables were compared using the χ^2 test or Fisher's exact test. For continuous data, group comparisons were performed using an unpaired t test or the Mann-Whitney U test. Results were considered statistically significant if the two sided *P*-value was ≤ 0.05.

Results

Inhibition of CCR2 ameliorates inflammation after AMI

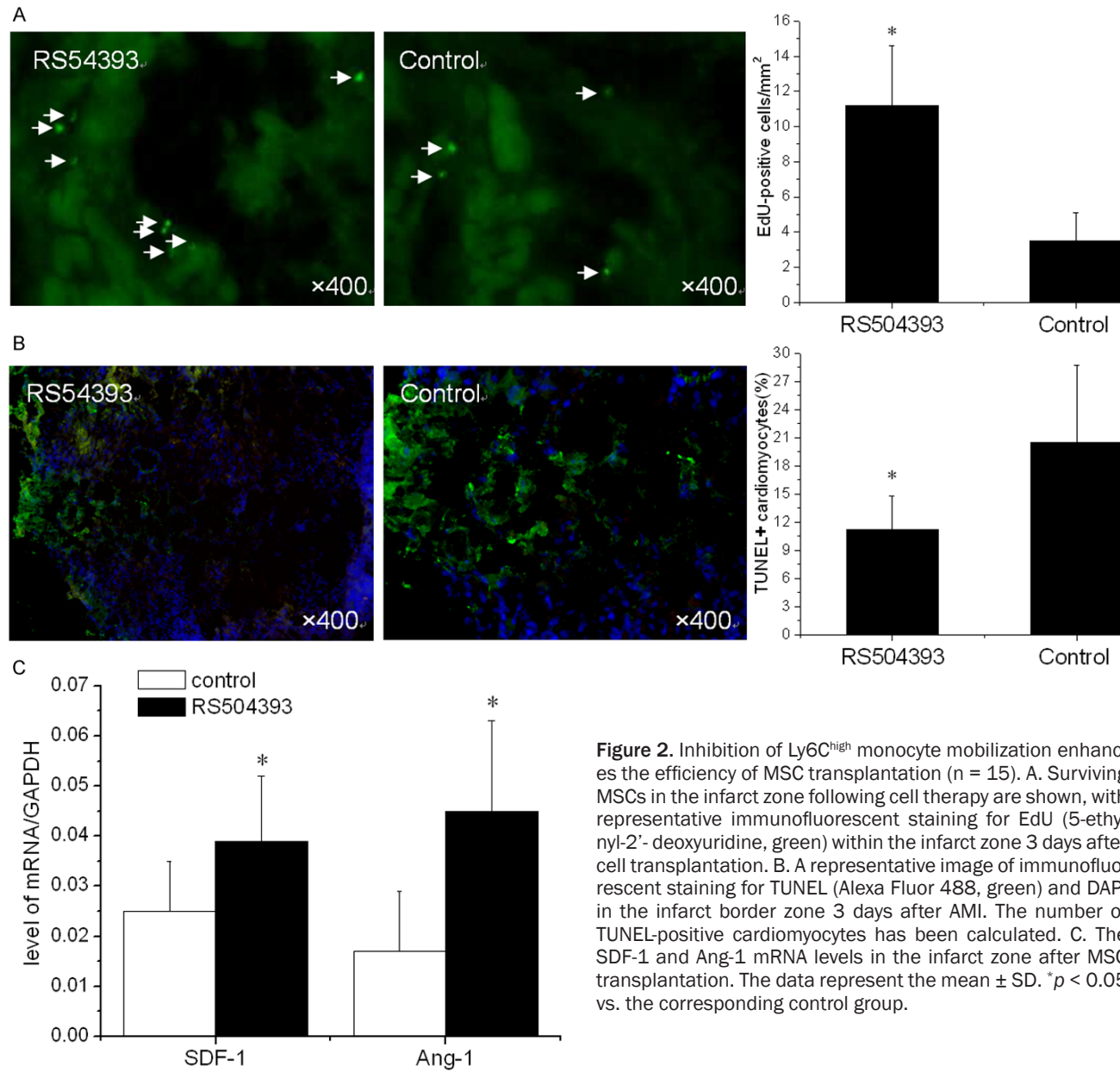Ly6C^{high} monocytes are potent inflammatory mediators and are a predominant source of

Figure 2. Inhibition of Ly6C^high monocyte mobilization enhances the efficiency of MSC transplantation (n = 15). A. Surviving MSCs in the infarct zone following cell therapy are shown, with representative immunofluorescent staining for EdU (5-ethynyl-2'- deoxyuridine, green) within the infarct zone 3 days after cell transplantation. B. A representative image of immunofluorescent staining for TUNEL (Alexa Fluor 488, green) and DAPI in the infarct border zone 3 days after AMI. The number of TUNEL-positive cardiomyocytes has been calculated. C. The SDF-1 and Ang-1 mRNA levels in the infarct zone after MSC transplantation. The data represent the mean ± SD. $^*p < 0.05$ vs. the corresponding control group.
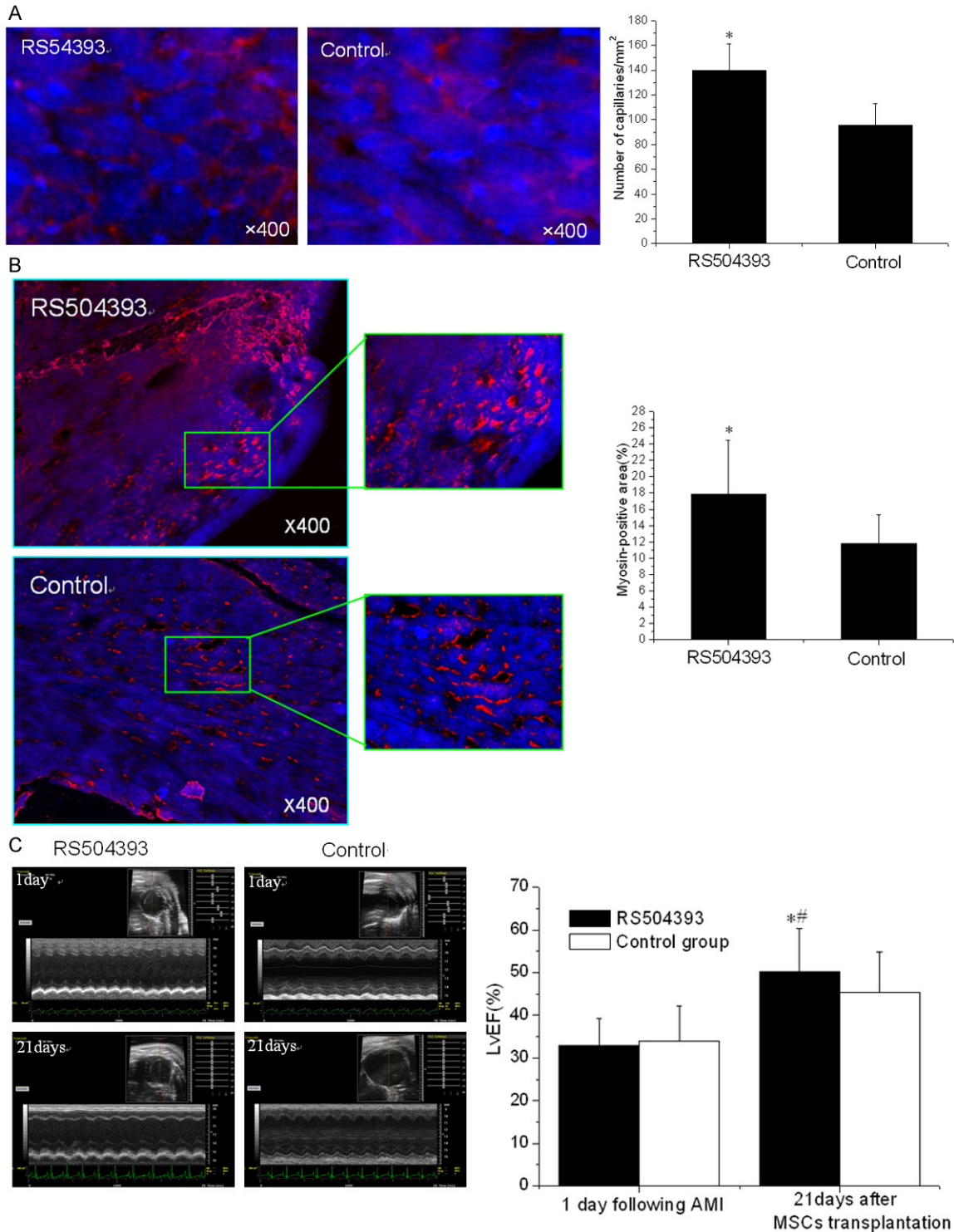
Figure 3. Reduced myocardial remodeling at three weeks (n = 15). A. The vascular density was determined using immunofluorescent staining for WGA (wheat germ agglutinin, red) and DAPI (blue) in the infarct zone 21 days post-MSC transplantation. B. A confocal image of representative immunofluorescent staining for cardiac myosin heavy chain (eFluor® 660, red) and DAPI (blue) within the infarct zone 21 days post-MSC transplantation. C. The ejection fraction at baseline and 21 days post-MSC transplantation. $^{*}p < 0.05$ vs. the corresponding control group at 21 days; $^{#}p < 0.05$ vs. the corresponding control group at 1 day post-AMI.

inflammation after AMI. We tested the deployment of Ly6C^{high} monocytes one day after AMI with the administration of RS504393 (2 mg/kg, subcutaneously). Flow cytometry analysis showed a significant reduction in circulating inflammatory Ly6C^{high} monocytes (22.02% ± 7.05% vs. 35.87% ± 13.04%, p < 0.001) one day after AMI in the mice treated with RS504393 compared to the control group (**Figure 1A**). CD11b positive monocytes in the infarcts at this time were further examined, and the results revealed significantly reduced numbers of cells compared to the groups not treated with RS504393 (42.34% ± 11.04% vs. 69.54% ± 18.5%, p < 0.001) (**Figure 1B**).

Increased survival of transplanted MSCs and decreased apoptosis of cardiomyocytes

Current limitations of MSC therapy include the impact of the inflammatory microenvironment on cellular behavior. We next evaluated the therapeutic potential of MSCs when CCR2 was inhibited by RS504393. After infarction, the hearts were harvested and embedded in paraffin. The sections were incubated with azide-conjugated Alexa Fluor 488. We observed a significant difference in EdU-positive cells (**Figure 2A**) in the infarction (11.2 ± 3.4/mm^2 vs. 3.5 ± 1.6/mm^2, p < 0.001) between the two groups three days after MSC transplantation. Consistent with the results for the restored MSCs, we also observed a significant reduction in TUNEL$^+$ cardiomyocytes (11.20% ± 3.55% vs. 20.51% ± 8.17%, p < 0.001) within the infarct zone compared to the control at three days (**Figure 2B**). In addition, increased levels of SDF-1（0.039 ± 0.013 vs. 0.022 ± 0.01, p < 0.001) and Ang-1 (0.045 ± 0.018 vs. 0.017 ± 0.12, p < 0.001) mRNA in the infarct zone were also detected (**Figure 2C**).

Increased vascular density and cardiac myosin-positive area after MSC transplantation

Three weeks after MSC infusion, the vascular density in the border zone of the infarction was examined using WGA (**Figure 3A**). A significant increase in the number of capillaries and small arterioles was observed in the RS504393 group (139.6 ± 21.7/mm^2 vs. 95.4 ± 17.6/mm^2, p < 0.001). Consistent with the increased vascular density results, a significant increase of the cardiac myosin-positive area within the infarct zone in the RS504393 group (17.9% ±

6.6% vs. 11.8% ± 3.5%, p < 0.001) was also observed (**Figure 3B**). Finally, the LV (LvEF %) remodeling at three weeks after MSC infusion was measured and was significantly ameliorated compared to the control (50.17 ± 10.06 vs. 45.44 ± 9.45, p < 0.001) (**Figure 3C**). Taken together, these data demonstrate that Ly6C^{high} monocytes play an adverse role in MSC transplantation post-AMI.

Decreased SDF-1 secretion by MSCs co-cultured with Ly6C^{high} monocytes

Studies demonstrated [14, 15] that the local trophic effects of MSC require cardiac progenitor cells and the expression of CM-CXCR4 and are also mediated by MSC stromal cell-derived factor-1 (SDF-1) secretion. After determining the levels of cytokines, including IL-1 (139.45 ± 30.44 vs. 80.05 ± 19.33, p < 0.001), IL-6 (187.82 ± 40.43 vs. 135.5 ± 22.09, p < 0.001), TNF-α (121.77 ± 31.65 vs. 75.3 ± 22.14, p < 0.001) and IFN-γ (142.46 ± 27.55 vs. 88.25 ± 19.91, p < 0.001) derived from the Ly6C$^{high/low}$ monocytes (**Figure 4A**), transwell chambers were used to examine the interactions between the cells. We observed that the SDF-1 secreted by the MSCs significantly decreased (280.77 ± 39.02 pg/ml vs. 435.5 ± 77.41 pg/ml, p < 0.001) when co-cultured with Ly6C^{high} monocytes compared to the Ly6C^{low} monocytes (**Figure 4B**). After co-culture with the Ly6C^{high} monocytes for 24 h, the cell viability of the co-cultured MSCs was determined using MTT (0.34 ± 0.06 vs. 0.71 ± 0.1, p < 0.001) and JC-1 mitochondrial membrane potential detection kits (0.45 ± 0.11 vs. 3.4 ± 0.3, p < 0.001). The results revealed the significantly decreased viability of the cells at this time compared to the control (**Figure 4C**).

Discussion

The unique properties of MSCs [16, 17], which include easy isolation and amplification from the bone marrow, immunological tolerance of allogeneic transplantation and multilineage potential, have led to their extensive investigation as a cell-based therapeutic strategy for cardiac repair. Although the causes of the decreased survival of transplanted MSCs have not yet been fully elucidated, inflammation, oxidative stress, and mitochondrial and energy metabolism dysfunction have been recognized as influential factors [18]. Current stem cell

sets, primarily oppose wound healing and contribute to left ventricular dilatation. In the setting of AMI, after these monocytes are recruited to the infarcted myocardium, they will release inflammatory mediators, such as TNF-α, IL-1/6, IFN-γ, inducible nitrous oxide synthase (iNOS) and matrix metalloproteinases (MMPs) [26]. Therefore, we conclude that the excessive inflammatory monocytes and the potent inflammatory microenvironment in the infarct are key factors that decrease the efficiency of stem cell transplantation.

Conclusion

We conclude that the mobilization of Ly6C^{high} monocytes after AMI negatively affect the local trophic effects of transplanted MSCs, which may occur because the over-expressed TNF-α, IL-1/6, and INF-γ by the Ly6C^{high} monocytes decreases the survival of MSCs and the subsequent secretion of SDF-1.

Acknowledgements

Disclosure of conflict of interest

None.

Address correspondence to: Dr. Genshan Ma, Department of Cardiology, Zhongda Hospital Affiliated with Southeast University, 89#, Dingjiaqiao Road, Nanjing 210009, China. E-mail: magenshanseu@126.com; magenshan@hotmail.com

References

[1] Rahbarghazi R, Nassiri SM, Ahmadi SH, Mohammadi E, Rabbani S, Araghi A, Hosseinkhani H. Dynamic induction of pro-angiogenic milieu after transplantation of marrow-derived mesenchymal stem cells in experimental myocardial infarction. Int J Cardiol 2014; 173: 453-66.

[2] Pasternak J. Cardiac stem cells and their clinical use. Einstein (Sao Paulo) 2014; 12: 134-5.

[3] Matar AA, Chong JJ. Stem cell therapy for cardiac dysfunction. Springerplus 2014; 3: 440.

[4] Goichberg P, Chang J, Liao R, Leri A. Cardiac stem cells: biology and clinical applications. Antioxid Redox Signal 2014; 21: 2002-17.

[5] Hayashi E, Hosoda T. Myocyte renewal and therapeutic myocardial regeneration using various progenitor cells. Heart Fail Rev 2014; 19: 789-97.

[6] Kamei M, Carman CV. New observations on the trafficking and diapedesis of monocytes. Curr Opin Hematol 2010; 17: 43-52.

[7] Ghosh M, Gerber C, Rahman MM, Vernier KM, Pereira FE, Subramani J, Caromile LA, Shapiro LH. Molecular mechanisms regulating CD13-mediated adhesion. Immunology 2014; 142: 636-47.

[8] Cochain C, Auvynet C, Poupel L, Vilar J, Dumeau E, Richart A, Récalde A, Zouggari Y, Yin KY, Bruneval P, Renault G, Marchiol C, Bonnin P, Lévy B, Bonecchi R, Locati M, Combadière C, Silvestre JS. The Chemokine Decoy Receptor D6 Prevents Excessive Inflammation and Adverse Ventricular Remodeling After Myocardial Infarction. Arterioscler Thromb Vasc Biol 2012; 32: 2206-13.

[9] Pedersen TO, Blois AL, Xue Y, Xing Z, Sun Y, Finne-Wistrand A, Lorens JB, Fristad I, Leknes KN, Mustafa K. Mesenchymal stem cells induce endothelial cellquiescence and promote capillary formation. Stem Cell Res Ther 2014; 5: 23.

[10] Ning H, Albersen M, Lin G, Lue TF, Lin CS. Effects of EdU Labeling on Mesenchymal Stem Cells. Cytotherapy 2013; 15: 57-63.

[11] Lin G, Huang YC, Shindel AW, Banie L, Wang G, Lue TF, Lin CS. Labeling and Tracking of Mesenchymal Stem Cells with EdU. Cytotherapy 2009; 11: 864-73.

[12] Sheng Z, Yao Y, Li Y, Yan F, Huang J, Ma G. Bradykinin Preconditioning Improves Therapeutic Potential of Human Endothelial Progenitor Cells in Infarcted Myocardium. PLoS One 2013; 8: e81505.

[13] Yan F, Yao Y, Chen L, Li Y, Sheng Z, Ma G. Hypoxic Preconditioning Improves Survival of Cardiac Progenitor Cells: Role of Stromal Cell Derived Factor-1a-CXCR4 Axis. PLoS One 2012; 7: e37948.

[14] Rueda P, Richart A, Récalde A, Gasse P, Vilar J, Guérin C, Lortat-Jacob H, Vieira P, Baleux F, Chretien F, Arenzana-Seisdedos F, Silvestre JS. Homeostatic and Tissue Reparation Defaults in Mice Carrying Selective Genetic Invalidation of CXCL12/Proteoglycan Interactions. Circulation 2012; 126: 1882-95.

[15] Zhao S, Chang SL, Linderman JJ, Linderman JJ, Feng FY, Luker GD. A Comprehensive Analysis of CXCL12 Isoforms in Breast Cancer1, 2. Transl Oncol 2014; S1936-5233: 00021-7.

[16] Williams AR, Hare JM. Mesenchymal Stem Cells Biology, Pathophysiology, Translational Findings, and Therapeutic Implications for Cardiac Disease. Circ Res 2011; 109: 923-40.

[17] Alfaro MP, Young PP. Lessons from genetically altered mesenchymal stem cells (MSCs): can-

didates for improved MSC-directed myocardial repair. Cell Transplant 2012; 21: 1065-74.

[18] Cejkova J, Trosan P, Cejka C, Lencova A, Zajicova A, Javorkova E, Kubinova S, Sykova E, Holan V. Suppression of alkali-induced oxidative injury in the cornea by mesenchymal stem cells growing on nanofiber scaffolds and transferred onto the damaged corneal surface. Exp Eye Res 2013; 116: 312-23.

[19] Reichert JC, Schmalzl J, Prager P, Gilbert F, Quent VM, Steinert AF, Rudert M, Nöth U. Synergistic effect of Indian hedgehog and bone morphogenetic protein-2 gene transfer to increase the osteogenic potential of human mesenchymal stem cells. Stem Cell Res Ther 2013; 4: 105.

[20] Tomoaki Kudo, Masayuki Kubo, Shunsaku Katsura, Arata Nishimoto, Koji Ueno, Makoto Samura, Yasuhiko Fujii, Tohru Hosoyama, Kimikazu Hamano. Hypoxically preconditioned human peripheral blood mononuclear cells improve blood flow in hindlimb ischemia xenograft model. Am J Transl Res 2014; 6: 570-579.

[21] Sharven Taghavi, Jon C George. Homing of stem cells to ischemic myocardium. Am J Transl Res 2013; 5: 404-411.

[22] Maxson S, Lopez EA, Yoo D, Danilkovitch-Miagkova A, Leroux MA. Concise review: role of mesenchymal stem cells in wound repair. Stem Cells Transl Med 2012; 1: 142-9.

[23] Deschepper M, Oudina K, David B, Myrtil V, Collet C, Bensidhoum M, Logeart-Avramoglou D, Petite H. Survival and function of mesenchymal stem cells (MSCs) depend on glucose to overcome exposure to long-term, severe and continuous hypoxia. J Cell Mol Med 2011; 15: 1505-14.

[24] Das R, Jahr H, van Osch GJ, Farrell E. The role of hypoxia in bone marrow-derived mesenchymal stem cells: considerations for regenerative medicine approaches. Tissue Eng Part B Rev 2010; 16: 159-68.

[25] Hadad I, Veithen A, Springael JY, Sotiropoulou PA, Mendes Da Costa A, Miot F, Naeije R, De Deken X, Entee KM. Stroma cell-derived factor-1α signaling enhances calcium transients and beating frequency in rat neonatal cardiomyocytes. PLoS One 2013; 8: e56007.

[26] Ley K, Miller YI, Hedrick CC. Monocyte and macrophage dynamics during atherogenesis. Arterioscler Thromb Vasc Biol 2011; 31: 1506-16.

[27] Zhu B, Kennedy JK, Wang Y, Sandoval-Garcia C, Cao L, Xiao S, Wu C, Elyaman W, Khoury SJ. Plasticity of Ly-6C(hi) myeloid cells in T cell regulation. J Immunol 2011; 187: 2418-32.

[28] Robbins CS, Chudnovskiy A, Rauch PJ, Figureueiredo JL, Iwamoto Y, Gorbatov R, Etzrodt M, Weber GF, Ueno T, van Rooijen N, Mulligan-Kehoe MJ, Libby P, Nahrendorf M, Pittet MJ, Weissleder R, Swirski FK. Extramedullary hematopoiesis generates Ly-6C (high) monocytes that infiltrate atherosclerotic lesions. Circulation 2012; 125: 364-74.